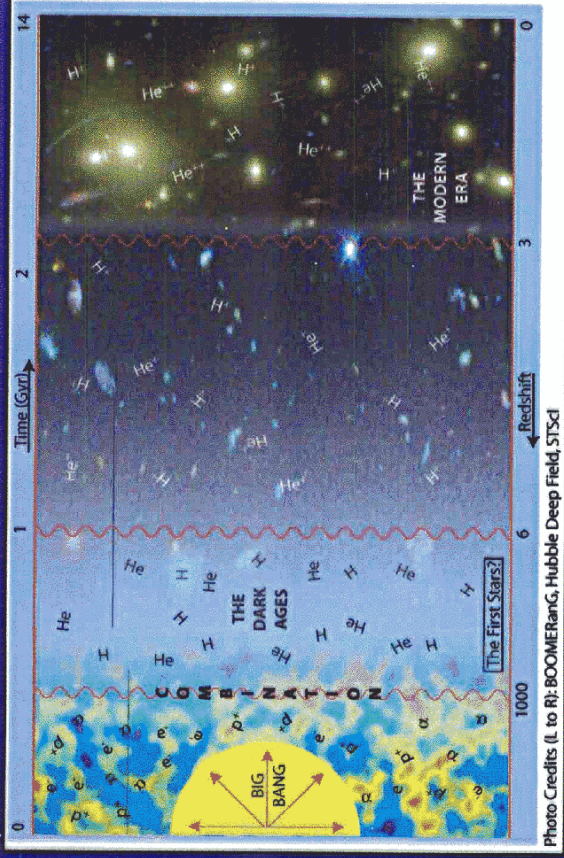
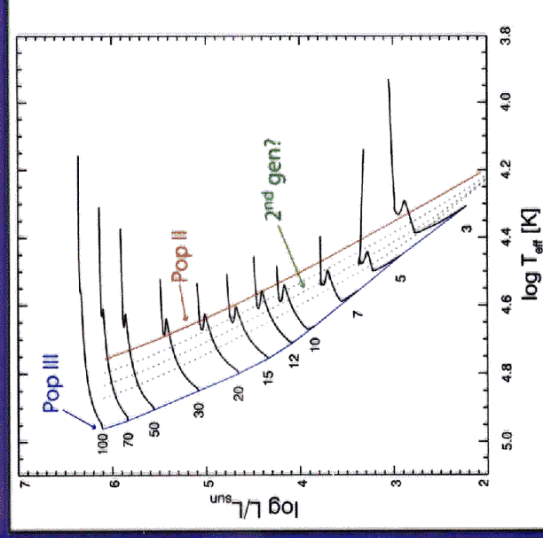


## Reionization and the "Dark Ages"



The period between the "combination" and the H reionization at  $z \sim 6$  is known as the "dark ages" - before the formation of galaxies and stars. In the common picture, H reionization is accomplished by stars at  $z > 6$ . The reionization of He is attributed to QSOs, which have harder ionizing spectra and reach a peak number density at  $z = 3$ .

## Evolving Models of Population III

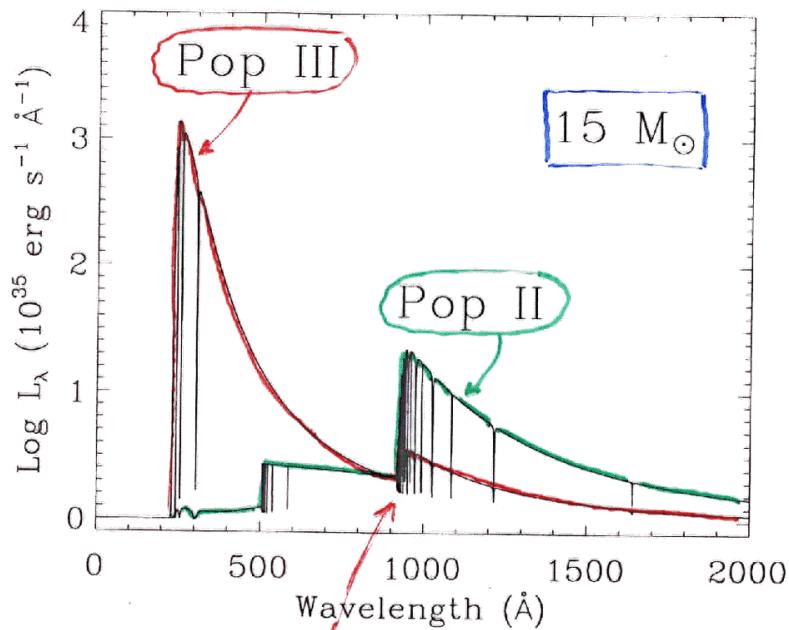


- Metal-free stars are 2x hotter and 5x smaller than their Pop II counterparts.
- In general, stars evolve off the MS to lower  $T_{\text{eff}}$  and higher  $L$ .
- Zero-age models with  $Z_c = 10^{-8}, 10^{-7},$  and  $10^{-6}$  lie between Pop III and Pop II (green). These may represent the 2<sup>nd</sup> generation.

ZERO-METALLICITY STARS AND THE EFFECTS OF THE FIRST STARS ON REIONIZATION

JASON TUMLINSON AND J. MICHAEL SHULL<sup>1</sup>

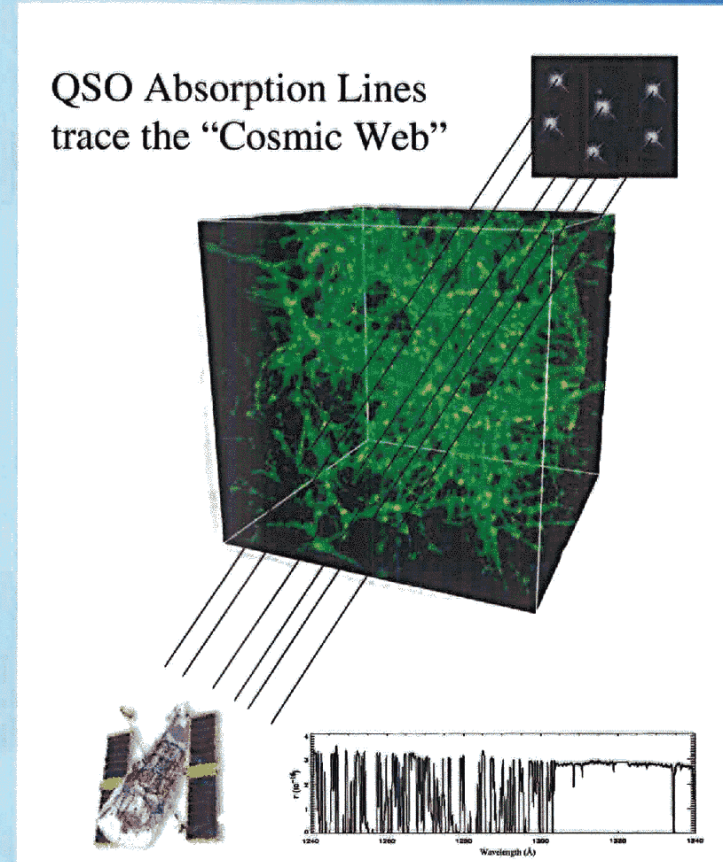
THE ASTROPHYSICAL JOURNAL, 528:L65-L68



Note The difference  
in Lyman breaks  
( $T_{\text{eff}}$  larger in Pop III)

# Large-scale Structure and the IGM

QSO Absorption Lines  
trace the "Cosmic Web"

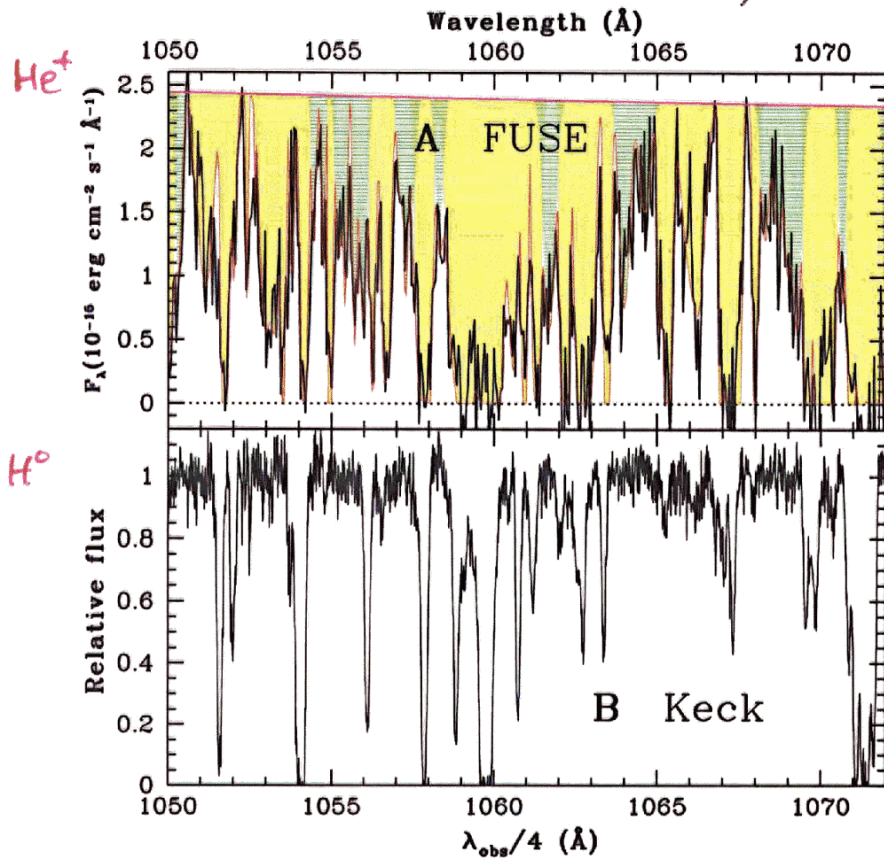


- Visualization concept from Schiminovich & Martin
- Numerical simulation from Cen & Ostriker (1998)
- Songaila et al. (1995) Keck spectrum adapted by Lindler & Heap

He II and HI Lyman $\alpha$  Forests

[2.3  $\leq$  z  $\leq$  2.9]

Kriss et al. 2001  
Shull et al 2004  
Zheng et al 2004



Fine-grained Variation

$\Delta z \sim 10^3$   
(Mpc-scale)

$$\eta = \frac{N(\text{He II})}{N(\text{H I})} = \frac{4 \tau_{\text{He II}}}{\tau_{\text{H I}}}$$

Shull et al. (2004) ApJ

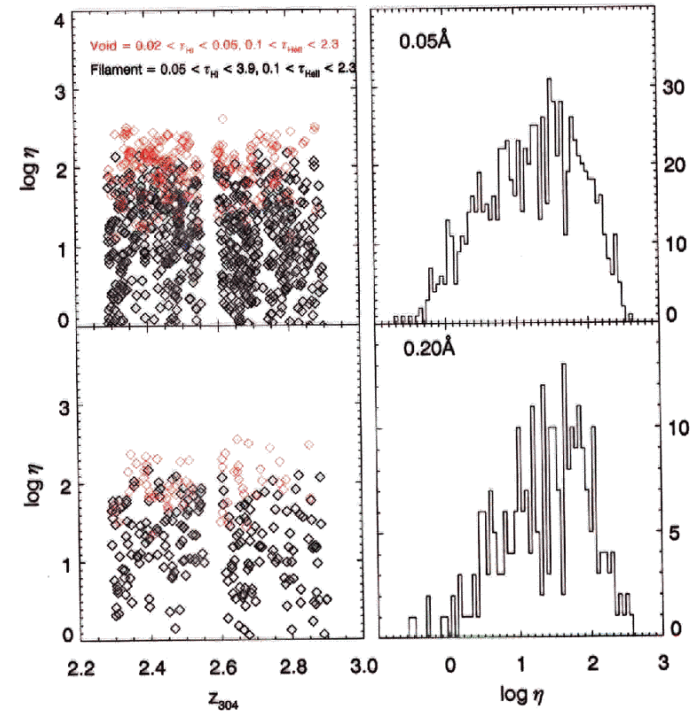
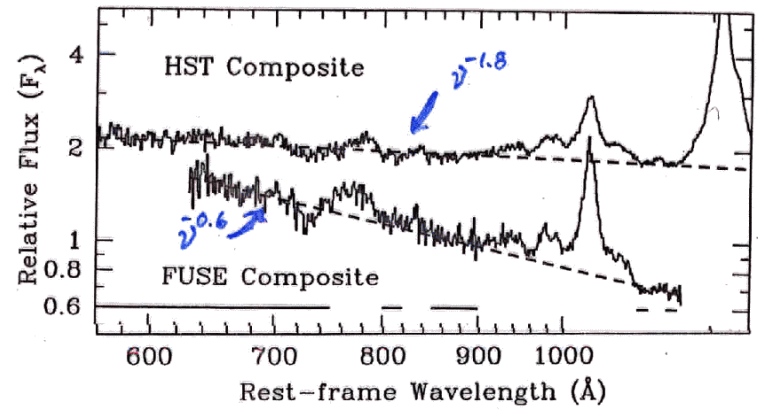
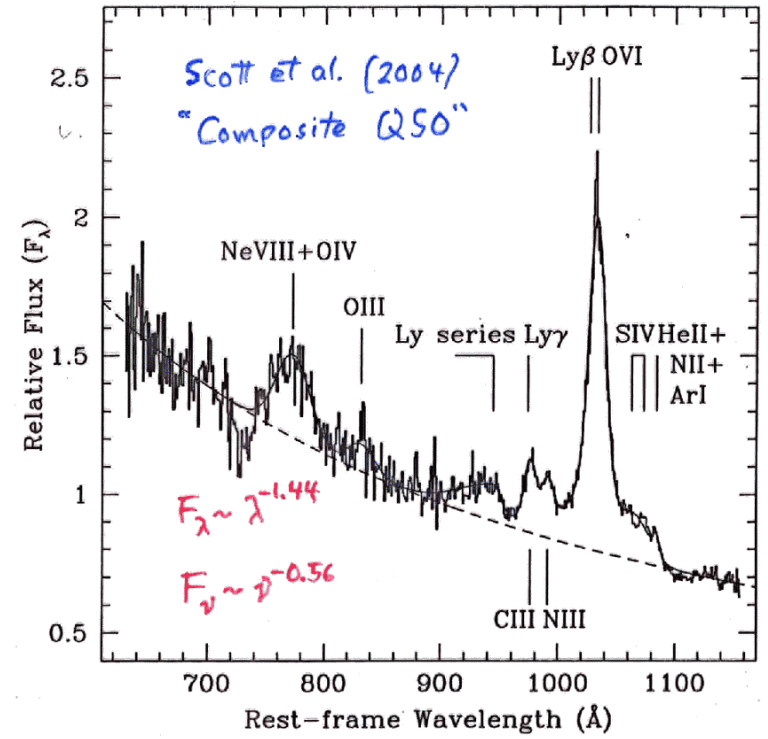
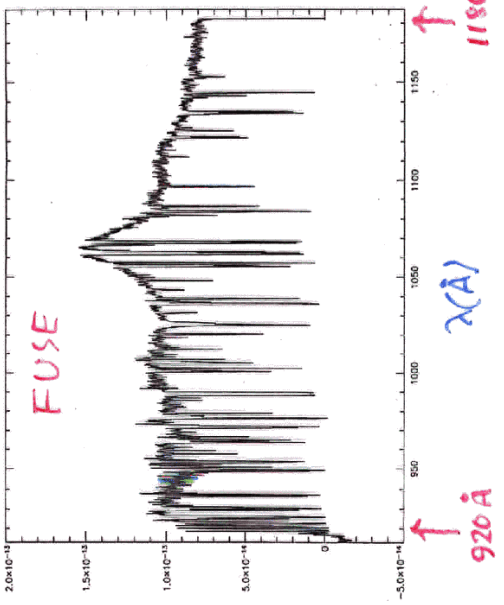
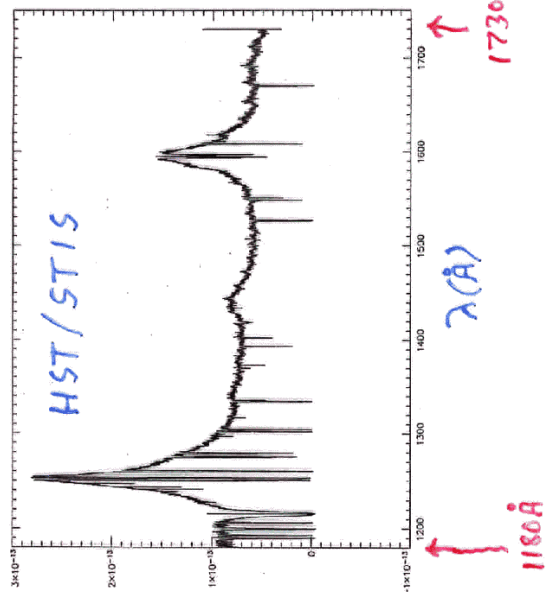
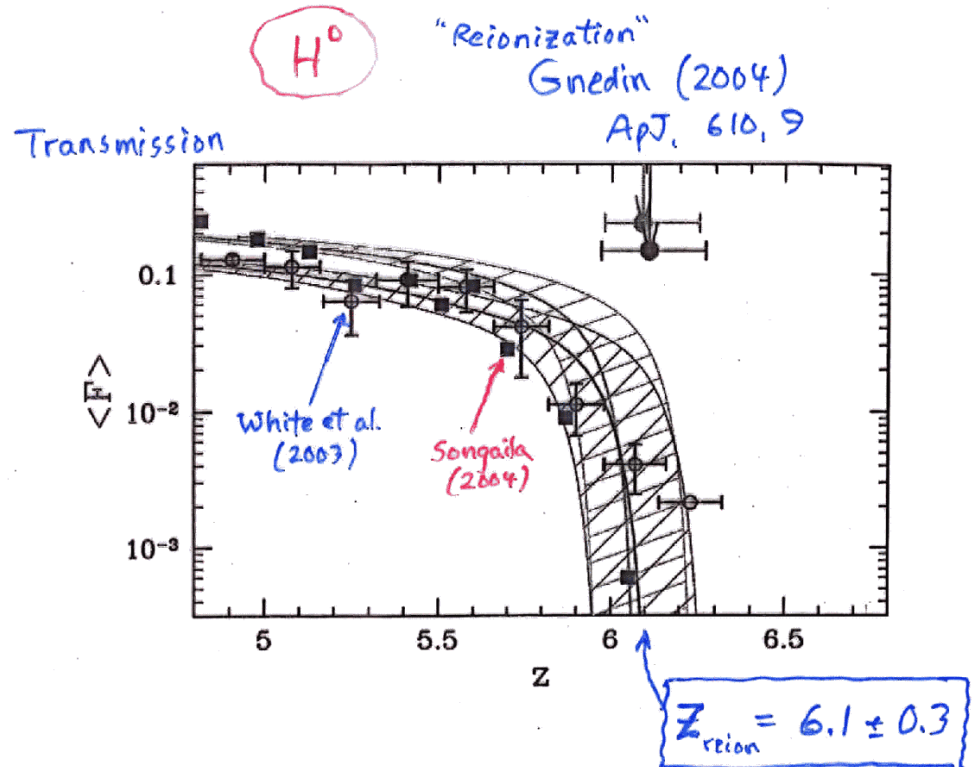
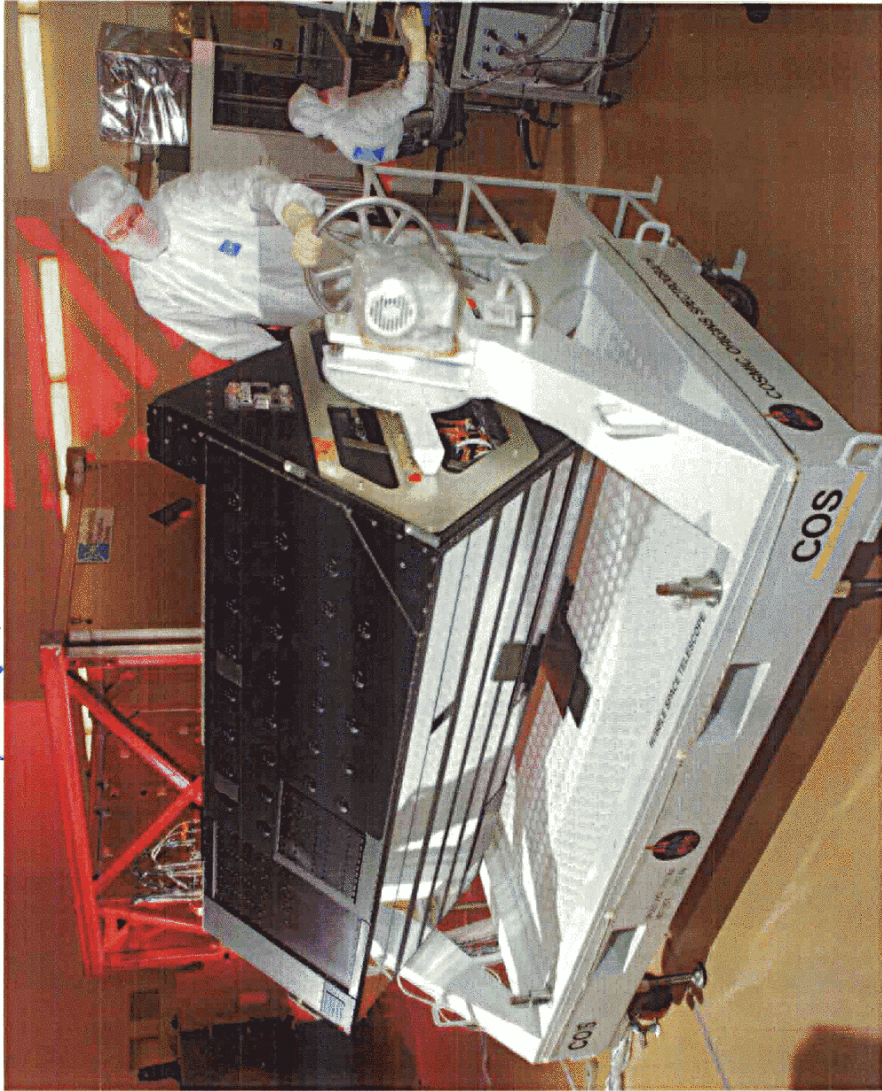


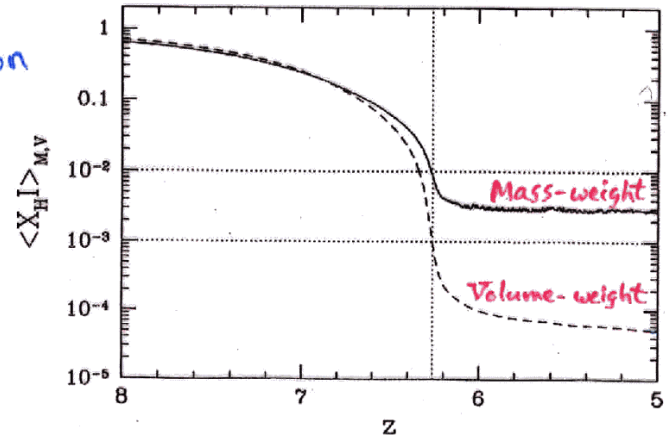
Fig. 3.— Left panels show the distribution with redshift of  $\eta = N(\text{He II})/N(\text{H I})$ , determined here as  $\eta = 4\tau_{\text{HeII}}/\tau_{\text{HI}}$ , in wavelength bins of 0.05 Å (top panels) and 0.20 Å (bottom panels). The distribution of  $\eta$ , integrated over  $2.3 < z < 2.9$  is shown in the right panels. With the accuracy of these data, we can reliably measure optical depths in the ranges  $0.1 < \tau_{\text{HeII}} < 2.3$  and  $0.02 < \tau_{\text{HI}} < 3.91$ . Gap at  $z = 2.6$  lies between the LiFa and LiF1b FUSE detector segments. “Filaments” in the Ly $\alpha$  forest are plotted in black ( $\tau_{\text{HI}} > 0.05$ ), while “voids” have  $0.02 < \tau_{\text{HI}} < 0.05$  and are plotted in red, some as lower limits. The large fluctuations in  $\eta$  suggest wide variation in the spectra of the ionizing sources, density fluctuations, or significant effects of radiative transfer in the IGM.



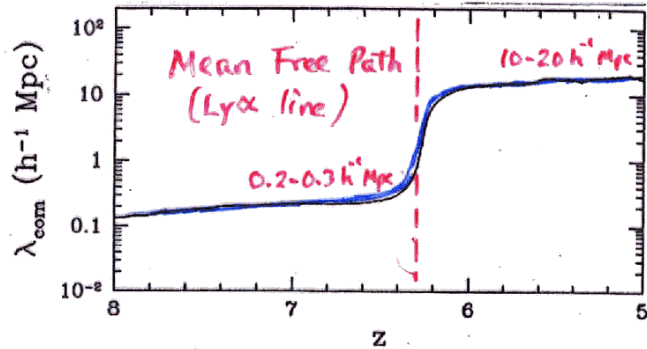
Future UV Spectrograph? COSMIC ORIGINS SPECTROGRAPH



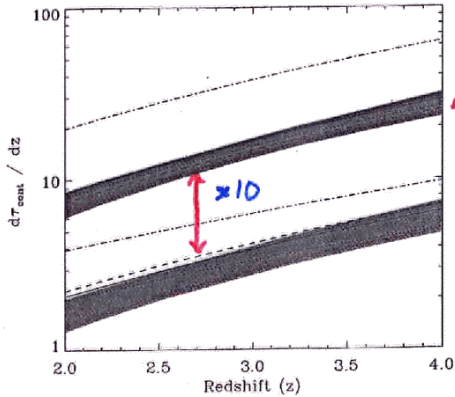
Neutral Fraction



Gnedin (2004)



Fardal, Giroux, & Shull (1998)



He II Opacity (Continuum)  $\left[ \frac{d\tau}{dz} \sim 10 \Rightarrow \Delta z \sim 0.1 \right]$  34 Mpc  
 H I Opacity (Continuum)  $\left[ \frac{d\tau}{dz} \sim 2 \Rightarrow \Delta z \sim 0.5 \right]$  180 Mpc

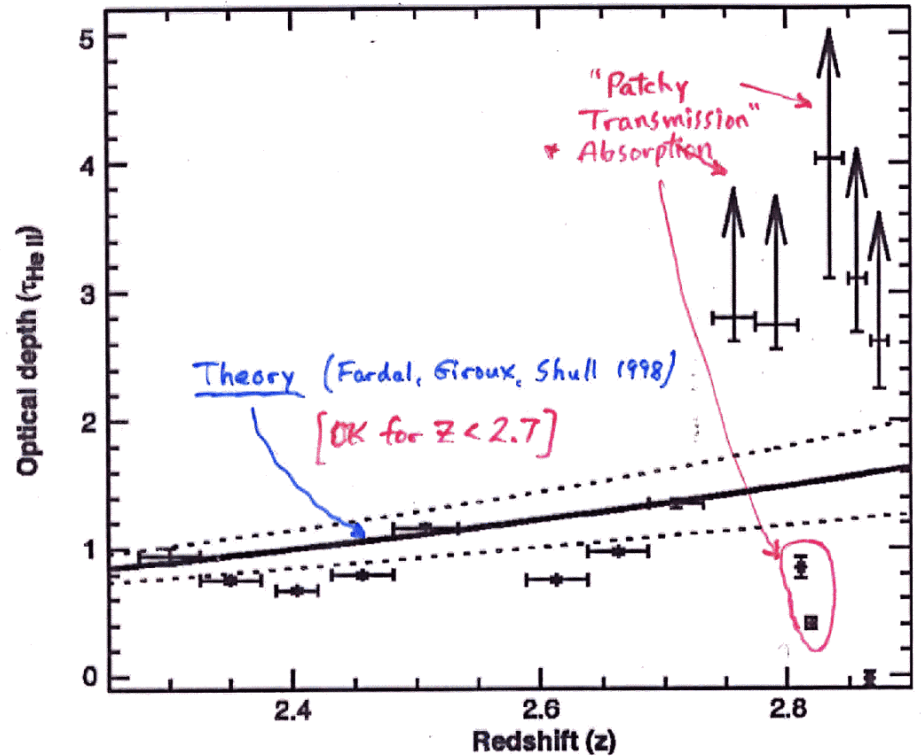
He II opacity  $\gg$  H I opacity

He<sup>+</sup> optical depth

[HE 2347-4342]

Kriss et al. 2001  
 Science 293, 1112

$Z_{em} = 2.885$ ,  $V = 16.1$  (Reimers et al. 1997)

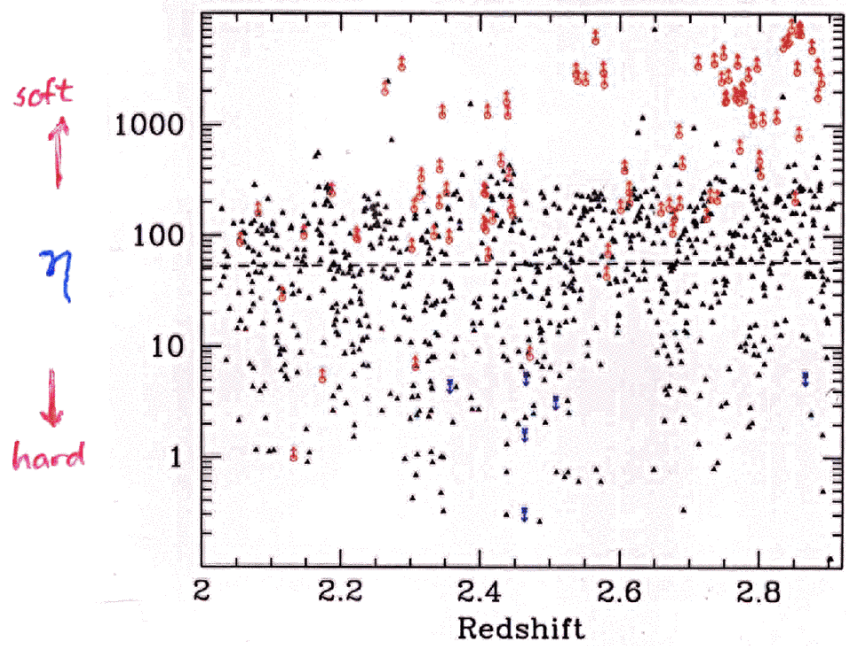


$$\eta = \frac{n_{\text{He III}}}{n_{\text{H II}}} \frac{\alpha_{\text{He II}}^{(A)}}{\alpha_{\text{H I}}^{(A)}} \frac{\Gamma_{\text{H I}}}{\Gamma_{\text{He II}}} \approx (1.70) \frac{J_{\text{H I}}}{J_{\text{He II}}} \frac{(3 + \alpha_4)}{(3 + \alpha_1)} T_{4.3}^{0.055}$$

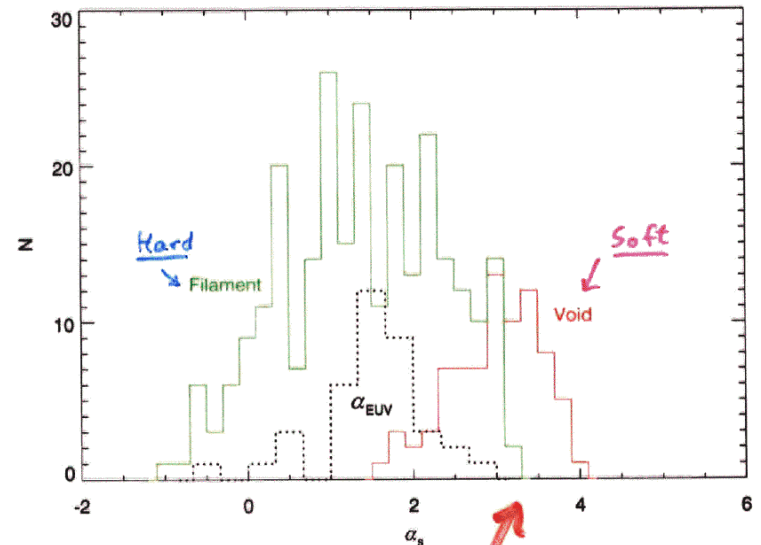
$\uparrow$   
 $4 + \alpha_{\text{eff}}$

$$\eta \equiv \frac{N(\text{He II})}{N(\text{H I})}$$

Shull et al. (2004) ApJ  
 Zheng et al (2004) ApJ



$\frac{\text{He II}}{\text{H I}}$  toward HE2347-4342 (FUSE + VLT)



Higher  $\eta$  (soft ioniz sources) in voids

- Not Pop III stars ( $\eta \sim 10$ )
- Probably RT effect + AGN (clumpy IGM)

Metagalactic Ionizing Background

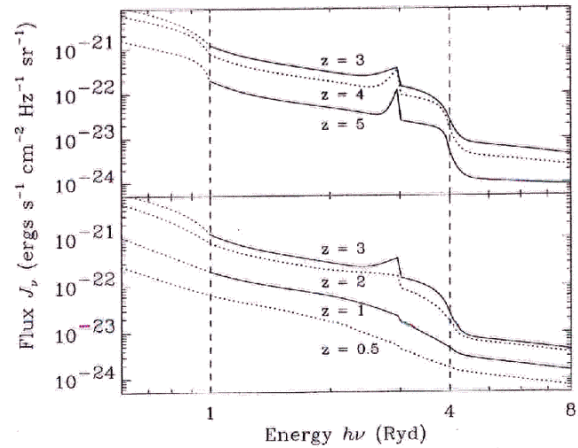
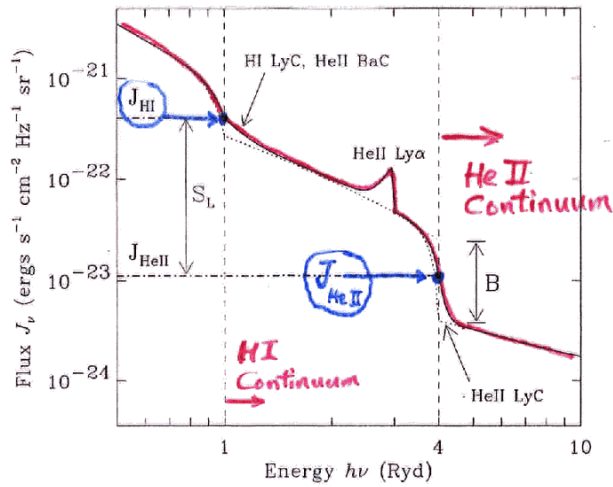


FIG. 7.—Evolution of the ionizing background with redshift, assuming quasar model Q2 with spectral index  $\alpha_s = 2.1$  and absorption model A2. Top,  $3 \leq z \leq 5$ ; bottom,  $0.5 \leq z \leq 3$ . See discussion in § 3.

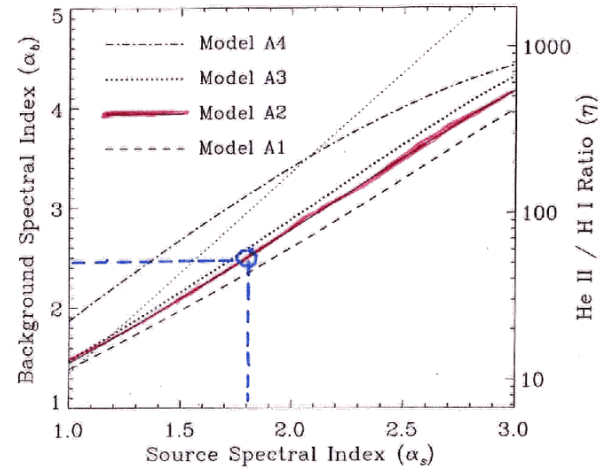


FIG. 10.—Dependence of the background spectral index  $\alpha_b$  upon the intrinsic spectral index  $\alpha_s$  of ionizing sources, for the four opacity models in the text, for quasar model Q1 and  $z = 3$ . The light dotted curve shows the analytic model,  $\alpha_b = 2.0\alpha_s - 0.64$ , of § 2.2. It is somewhat steeper than the numerical models, partly because it ignores the finite-density effects that affect models with soft spectra.



*ApJ*, 615, ~~in press~~ <sup>135</sup>

A Composite Extreme Ultraviolet QSO Spectrum from *FUSE*

Jennifer E. Scott<sup>1</sup>, Gerard A. Kriss<sup>1,2</sup>, Michael Brotherton<sup>3</sup>, Richard F. Green<sup>4</sup>, John Hutchings<sup>5</sup>, J. Michael Shull<sup>6</sup>, & Wei Zheng<sup>2</sup>

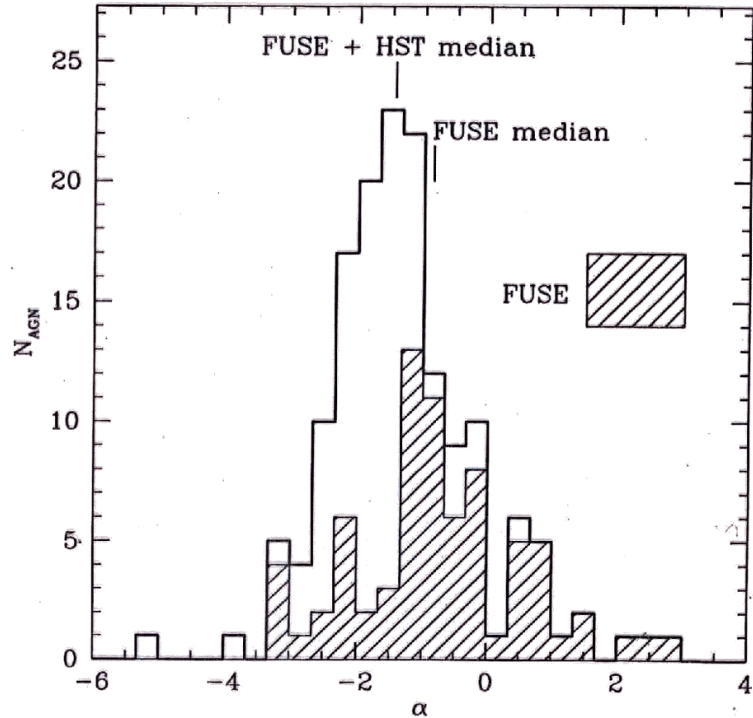
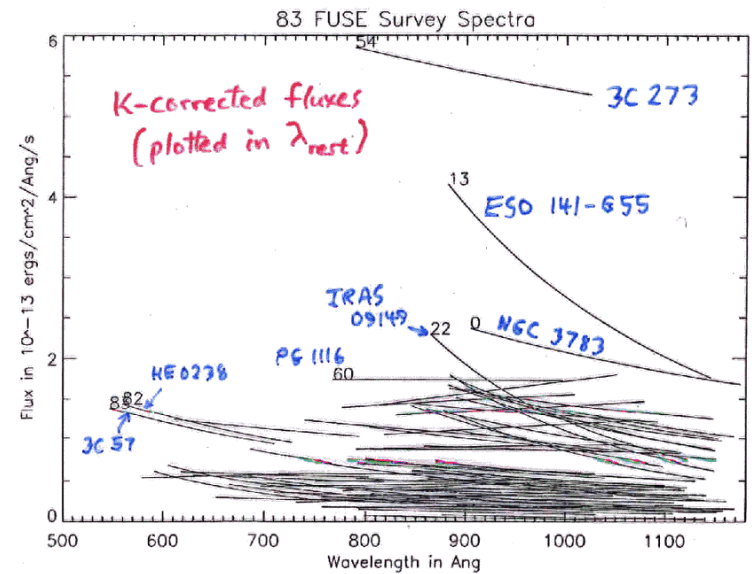
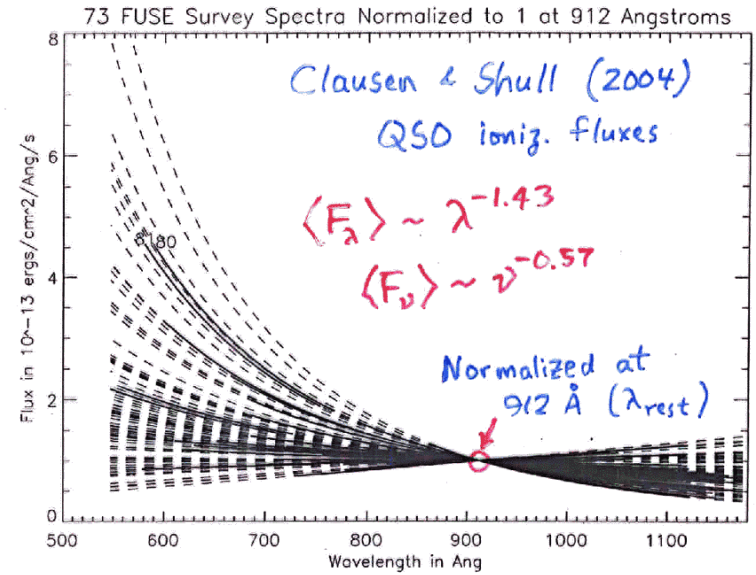
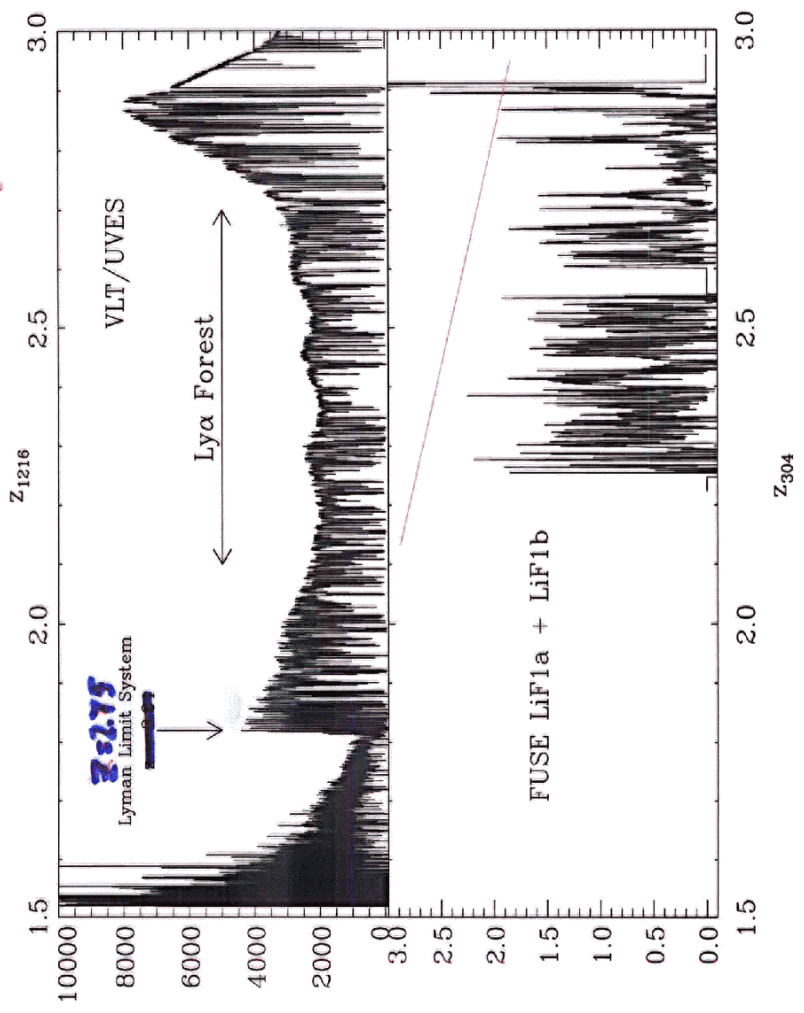


Fig. 12.— Histogram of EUV spectral slopes in *FUSE* sample and in the combined *FUSE* and *HST* sample.



VLT/UVES data (Reimers)  
on HI Ly $\alpha$



Shull, Tumlinson, et al. 2002

A STUDY OF THE REIONIZATION HISTORY OF INTERGALACTIC HELIUM WITH *FUSE* AND THE VERY LARGE TELESCOPE<sup>1</sup>

W. ZHENG,<sup>2</sup> G. A. KRISS,<sup>2,3</sup> J.-M. DEHARVENG,<sup>4</sup> W. V. DIXON,<sup>2</sup> J. W. KRUK,<sup>2</sup> J. M. SHULL,<sup>5,6</sup> M. L. GIROUX,<sup>7</sup>  
D. C. MORTON,<sup>8</sup> G. M. WILLIGER,<sup>2</sup> S. D. FRIEDMAN,<sup>3</sup> AND H. W. MOOS<sup>2</sup>

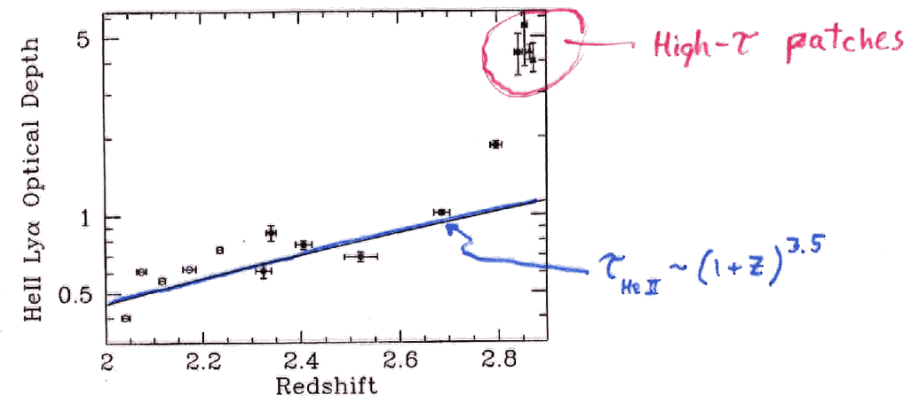


FIG. 10.—Redshift dependence of the He II Ly $\alpha$  opacity. Values below  $z = 2.3$  are derived from a line spectrum reconstructed from the fitted parameters that omit Ly $\beta$  and higher order Lyman lines. Between  $z = 2.3$  and  $2.7$  the values are direct measurements from the *FUSE* data, and at  $z > 2.7$  they are derived from the observed He II Ly $\beta$  absorption region. The curve representing  $\tau \propto (1+z)^{3.5}$  is plotted for comparison.

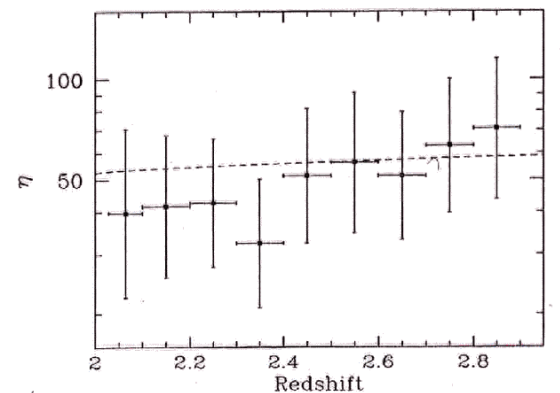


FIG. 8.—Column density ratio  $\eta$  vs. redshift. The average  $\eta$ -value is calculated from the components that are detected in both the *FUSE* and VLT spectra. The dashed curve represents the anticipated values if the ionizing sources are quasars with an EUV power law of  $f_\nu \propto \nu^{-1.7}$ , which are interpolated from results of Fardal et al. (1998).

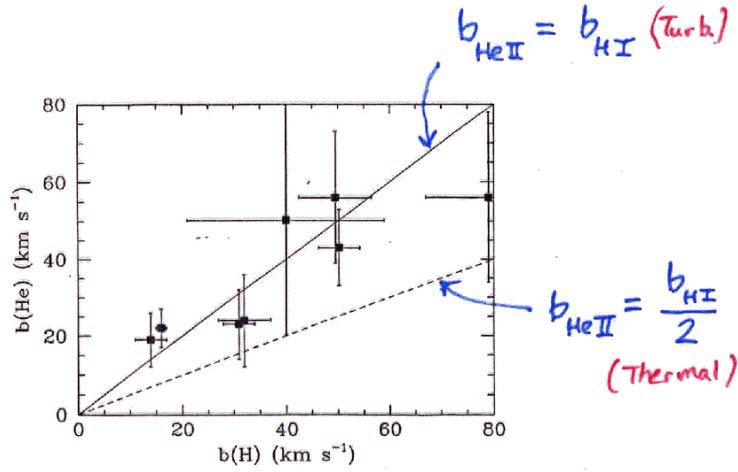
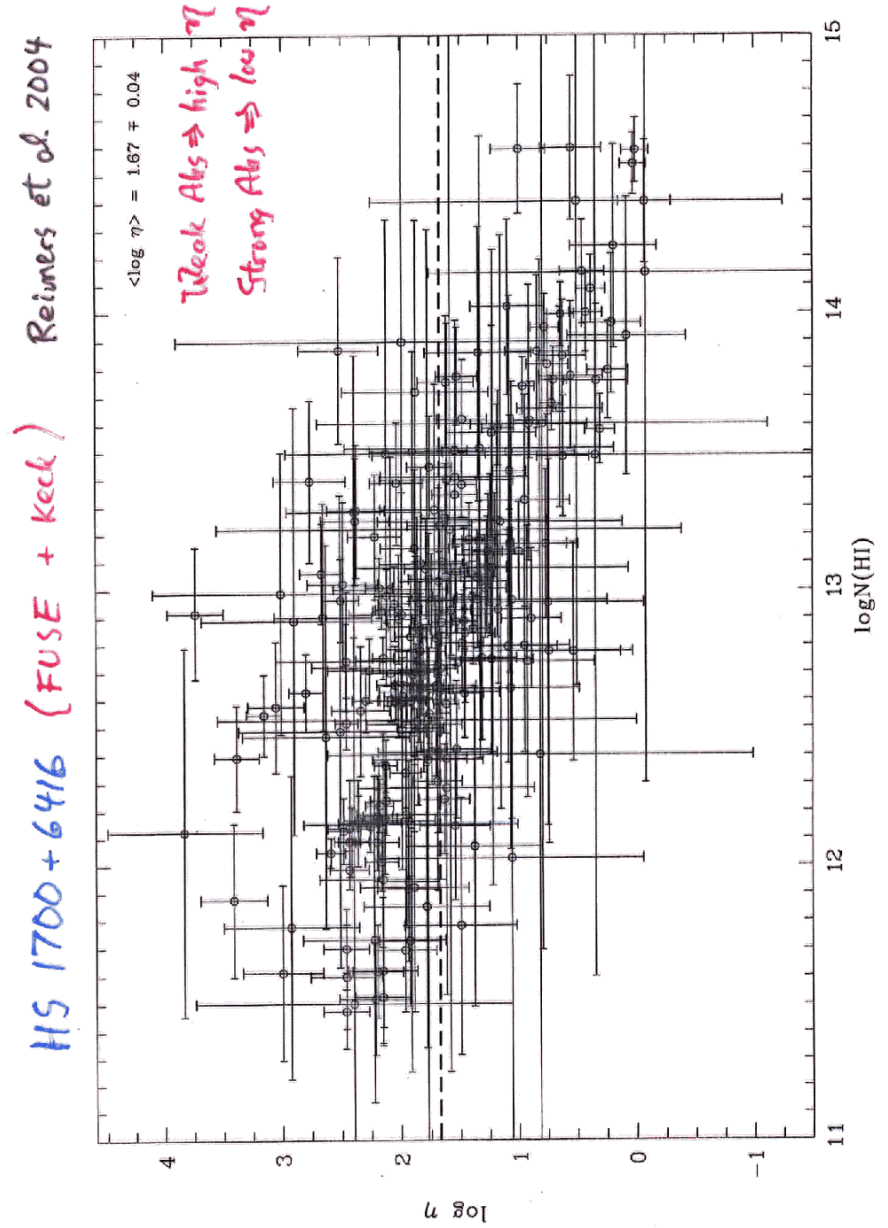
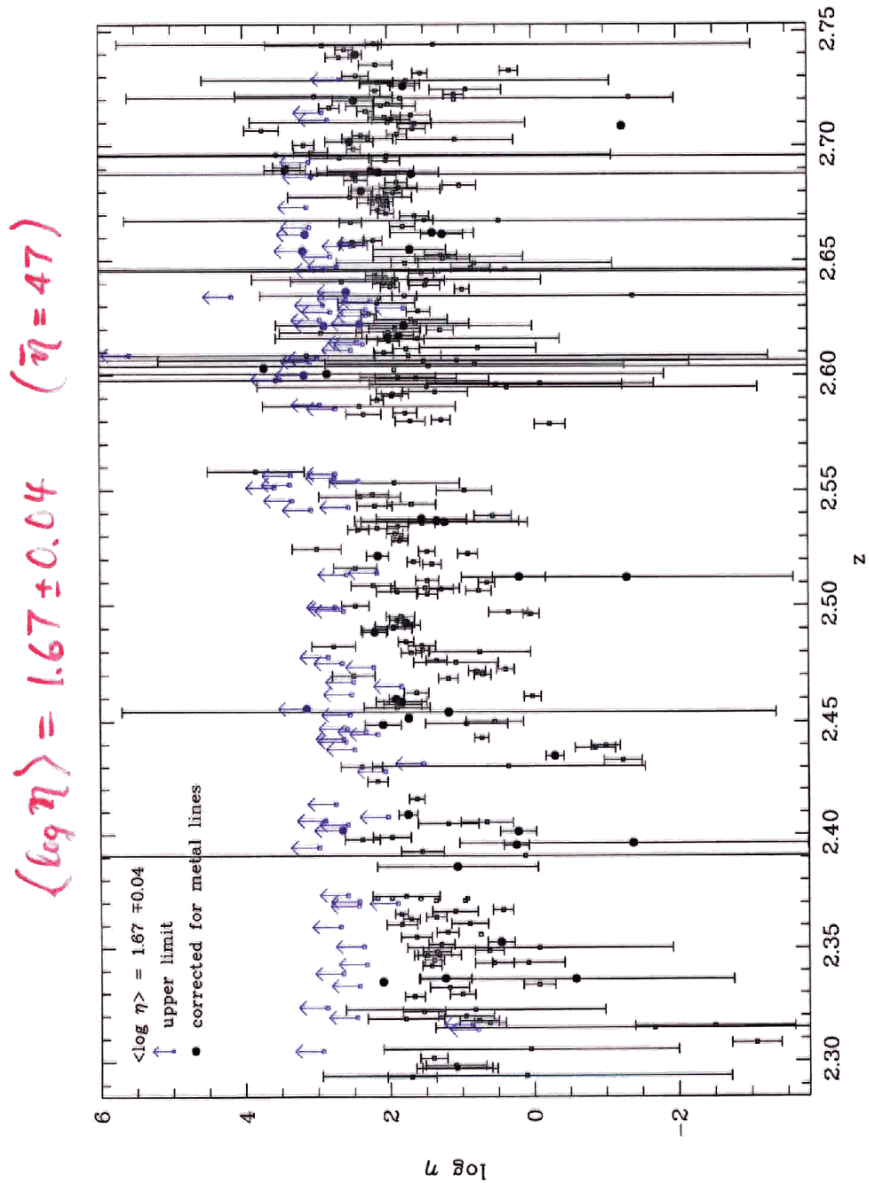


FIG. 6.—Doppler parameters for hydrogen and helium absorbers. The solid line stands for expected values with turbulence line-broadening, and the dashed line stands for thermal broadening.

best-fit:  $b_{\text{HeII}} = (0.95 \pm 0.12) b_{\text{HI}}$





WMAP [Kogut et al ; Spergel et al 2003]

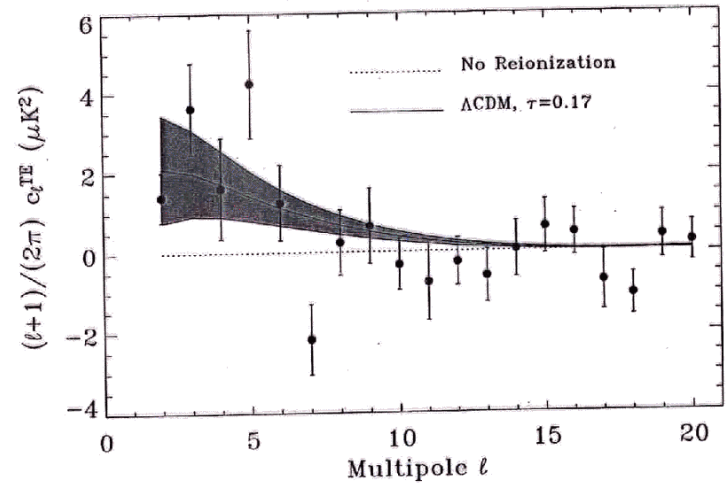
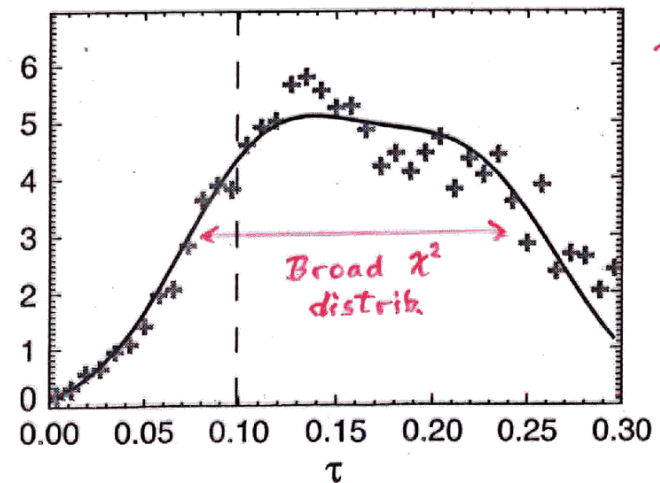


Fig. 8.— WMAP Polarization cross-power spectra  $c_l^{TE}$  (filled circles) compared to  $\Lambda$ CDM models with and without reionization. The rise in power for  $l < 10$  is consistent with reionization optical depth  $\tau = 0.17 \pm 0.04$ . The error bars on WMAP data reflect measurement errors only; adjacent points are slightly anti-correlated. The grey band shows the 68% confidence interval from cosmic variance. The value at  $l = 7$  is particularly sensitive to the foreground correction.



CMB Optical Depth

$$\tau_e = \int_0^{z_r} n_e \sigma_T \left( \frac{dl}{dz} \right) dz$$

$$\tau_e = \left( \frac{c}{H_0} \right) \left( \frac{2\Omega_b}{3\Omega_m} \right) \left[ \frac{\rho_{cr}(1-Y)(1+y)\sigma_T}{m_H} \right] \left[ \{\Omega_m(1+z_r)^3 + \Omega_\Lambda\}^{1/2} - 1 \right]$$

$$\approx (0.0376h) \left( \frac{\Omega_b}{\Omega_m} \right) \left[ \{\Omega_m(1+z_r)^3 + \Omega_\Lambda\}^{1/2} - 1 \right]$$

$$\tau_e \approx \left( \frac{c}{H_0} \right) \left( \frac{2\Omega_b}{3\Omega_m} \right) \left[ \frac{\rho_{cr}(1-Y)(1+y)\sigma_T}{m_H} \right] \Omega_m^{1/2} (1+z_r)^{3/2} \approx (0.00229)(1+z_r)^{3/2}$$

$$\Omega_b h^2 = 0.0224 \pm 0.0009$$

$$\Omega_m h^2 = 0.135^{+0.008}_{-0.009} \quad (\Omega_m + \Omega_\Lambda = 1)$$

$$Y_{He} = 0.244 \quad (\text{by mass})$$

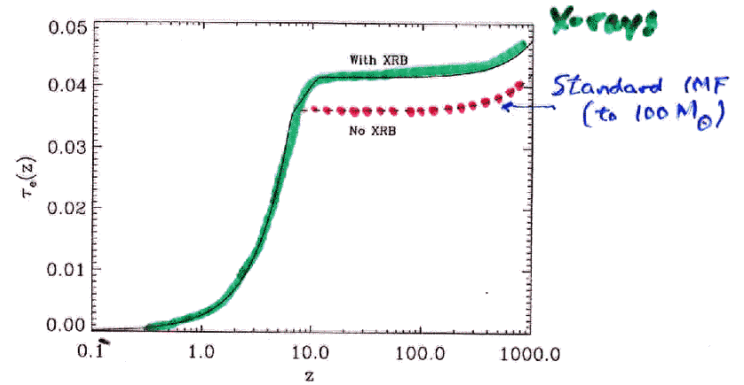
$$y_{He} = 0.0807 \quad (\text{by number})$$

$$(1+z_r) \approx (14.0) \left[ \frac{\tau_e}{0.12} \right]^{2/3}$$

Tegmark et al '04  
WMAP + Sloan

EXTENDED/PARTIAL/DOUBLE REIONIZATION

1. X-rays from Massive and Mini-QSOs



$$\tau_e \approx 0.04 - 0.05 \quad (\text{Standard IMF})$$

$$\approx 0.10 \quad (\text{High-Mass, Pop III stars})$$

Venkatesan, Giroux & Shull 2001: X-rays can cause significant preheating – up to  $10^4$  K – and partial ionization – up to 20% – prior to full reionization.

Residual electrons (freeze out from decoupling)

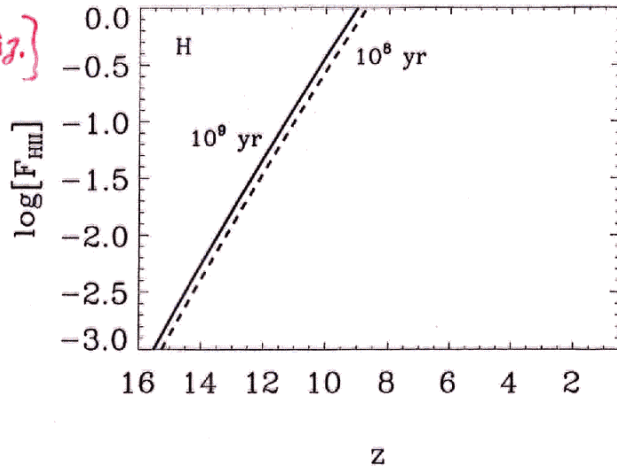
$$X_e \approx 10^{-3.3} \quad (\text{Seger et al. 2000})$$

$$\rightarrow \Delta\tau_e \approx (0.012) \left[ \frac{(1+z_r)}{500} \right]^{3/2}$$

VENKATESAN, TUMLINSON, & SHULL

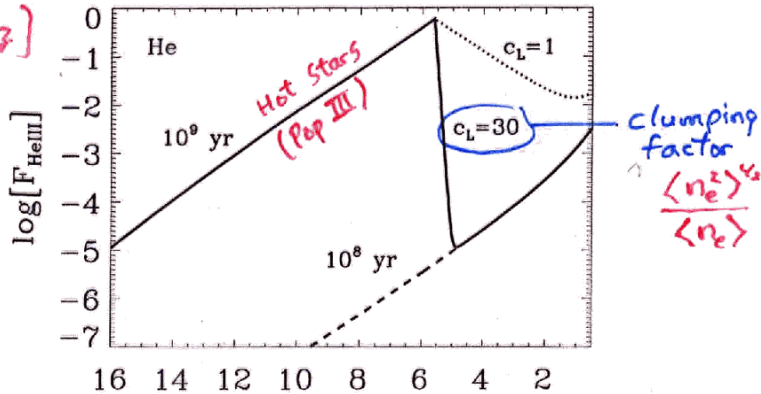
*ApJ* 584, 621  
(2003)

[H reioniz.]



"Double Reionization"?

[He<sup>+</sup> reioniz.]



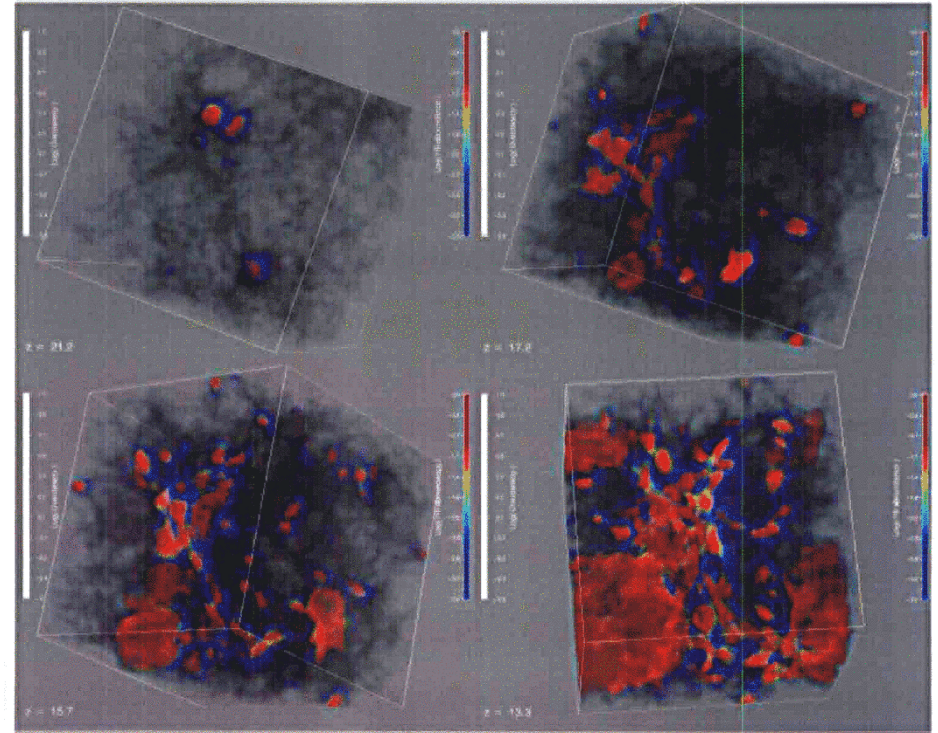
Metallicity?

$$Z_m \equiv \frac{(\rho_m/\rho_b)_{IGM}}{(\rho_m/\rho_b)_\odot} \approx (10^{-4}) \left[ \frac{z}{0.1 M_\odot \text{ yr}^{-1} \text{ Mpc}^{-3}} \right] \left[ \frac{t}{10^8 \text{ yr}} \right]$$

## Ionization Fronts (First Starbursts)

( $z \approx 10-20$ )

Ricotti et al. (2002)  
*ApJ*, 575, 49



$z = 15.7$

$z = 13.3$

